NIPES Journal of Science and Technology Research 4(1) 2022 pp.12 - 38 pISSN-2682-5821, eISSN-2682-5821

NIPES

Journal of Science and Technology Research

Journal homepage: www.nipesjournals.org.ng

Estimating Annual Amount of Soil Loss Over University of Benin Using RUSLE, GIS and Remote Sensing Methods

[a]Emeribe C.N, [b]Isagba E.S; [b]Iwhiwhu B.E; [a&c]Ogbomida E.T; [d]Akukwe T.I

[a*]National Centre for Energy and Environment, Energy Commission of Nigeria, University of Benin
[b]Department of Civil Engineering, Faculty of Engineering, University of Benin, Benin City, Edo State
[d]Directorate of Research, Innovation and Consultancy, the Copperbelt University, Riverside, Kitwe, Zambia [d]Department of Geography, University of Nigeria, Nsukka, Enugu State, Nigeria
*Corresponding Author: National Centre for Energy and Environment, Energy Commission of Nigeria, University of Benin, Benin City, Edo State, emeribe.c@ncee.org.ng +2348063581430

Article Info

Received 03 January. 2022
Revised 17 January 2022
Accepted 30 January 2022
Available online 05 March 2022

Keywords: *Gully erosion, Rainfall erosivity, soil erodibility, University of Benin, Soil loss*

https://doi.org/10.37933/nipes/4.1.2022.2

https://nipesjournals.org.ng

Abstract

The present study is aimed to estimate the annual soil loss of University of Benin gully. This was achieved by utilizing the Revised Universal Soil Loss Equation, RUSLE coupled with GIS Technique. A total of 15 samples were collected from the gully site, three at each chainage point. The soil analysis showed that the study area is highly sandy with low clay and silt content. This study area has very high infiltration rate, ranging from 93.64-2509.06 mm/hr. Result obtained for soil organic content revealed that organic matter content in the soil samples is small, ranging from 0.17 to a highest value of 2.30. Soil Erodibility ranges from 0.002 to 0.01ton·ha·hr/(ha·MJ·mm). This result is due to the soil texture being mainly sandy, as sand can be easily detached. On annual basis, the Rainfall-runoff erosivity value for the study area is very high. The study also found that Cover Management factor, C is low and uniform throughout the gully site. On the whole, the study found high annual soil loss, ranging from 1.509-7.545 ton/ha/yr. The maximum amount of estimated soil loss is determined as 7.545 ton per hectare per year which equals 75.45 kilogram per square kilometre per year (kg/sq. km/yr). Conservation planning and land use policies should be developed to focus on the more prone slopes, which are likely to suffer immensely from the directional influence of rainfall. The implementation of such an approach should be aimed at arresting directional rainfall erosion by the integration of various erosion control measures. Finally, dumping of refuse on the river channels and floodplains should be prohibited. Government and the University Management should enact and enforce laws to deter such activities.

1. Introduction

Soil erosion is a global environmental problem that affects the natural environment and agriculture productivity as well as causing soil degradation, sediment deposition, water quality degradation [1, 2]. Globally, it is estimated that erosion by water causes considerable soil fertility loss and decrease in productivity [3, 4]. The FAO-led Global Soil Partnership reports that globally and annually, 75 billion tonnes (Pg) of soil are eroded from arable lands, estimated at a financial loss of USD400 billion per year [5]. In Africa, past water erosion has been associated with 8.5% of mean yield loss [6]. A review of the global agronomic impact of soil erosion classified continents into two severity groups with Africa belonging to the more vulnerable group [7]. This is obvious in mostly the humid and sub-humid zones of Sub-Saharan Africa (SSA) where the annual soil loss given at over 50 tons ha−1 had been exacerbated by deforestation, population pressure and torrential downpours [8, 9]. This situation is not different in Nigeria which has witnessed rapid expansion in terms of population, urbanization and industrialization since independence in 1960. Such growth has been accompanied by changes of towns into major cities with numerous development projects involving land reclamation, housing schemes, highway constructions, and alternation of natural soil ecosystem among others. Studies have also revealed that gullies seem an urban phenomenon and has occurred at unparalleled rates resulting in huge social, economic and human losses in cities in southern Nigeria [10, 11, and 12].

The World Bank [13] recognized deforestation, water contamination, and soil degradation and loss as the three major environmental problems faced by Nigeria. Additionally, six others were specified: fishery loss, air pollution, coastal erosion, wildlife and biodiversity losses, gully erosion, and the spread of water hyacinth. Despite that these environmental problems affect know no boundary, some are however more prevalent in certain geographical regions of Nigeria. Gully erosion is a common environmental problem in southern Nigeria and caused an annual damage worth $100 million in 1990 in the country [14]. Some studies have estimated an average of 14862.8m^3 volume of soil loss to erosion from 1992 to 2002 [15, 16, 17]. In Edo State, Ehiorobo and Izinyon [14] monitored soil loss to erosion and found out that though gullies are usually striking, their small spatial extent usually make them unnoticeable in most low resolution imageries and available topographical maps. They also noted that because gully processes are not easy to study and the control os soil erosion difficult, gully erosions have been neglected. In the same light, [18] estimated that 329,436.5 and 531,417.6 tons of sediments were detached from gullies in Ikpoba and Auchi slope of Benin City respectively. There has been a continual soil loss over the University of Benin and to effectively tackle this problem, there is a need to evaluate the effects of contributing factors to soil erosion formation using Geographic Information Systems (GIS) and Remote Sensing (RS) techniques. This is especially as it has been noted that only little reliable data were available by the end of the 20th century both on the extent [9, 19] and on the cause-effect relationship between soil erosion and soil productivity [20, 6], but has been made easier by GIS and remote sensing that provide spatial information that is generally hard to acquire especially in developing countries [21, 22].

Studies on soil loss could be traced to the 1930s where its emphasis was majorly on its impact on agricultural productivity. During 1940 and 1956, USA research scientists developed a method for quantitative soil loss estimation. The soil loss equation had several factors, but agricultural practice and slope were considered primarily. Wischmeier and Smith [23] then developed the Universal Soil Loss Equation (USLE) using almost a decadal data collected from the National Runoff and Soil Loss Data Center, Purdue University in addition to previous studies. The USLE was a generally accepted mathematical model used to estimates the average annual soil loss of any study area. Over the years, [24] developed the Revised Universal Soil Loss Equation (RUSLE); an improvement of the USLE, which takes into cognizance both conservation practices and morphological factors. It has since then been used in the development of conservation planning and land-use decision making [2]. In the same light, this study sought to understand the character of some geomorphological factors in the development of soil erosion at the Ugbowo campus of the University of Benin, using the RUSLE with the aid of GIS and remote sensing techniques.

2. Methodology

2.1 Study area

The University of Benin gully site is located within the University of Benin, Benin City and geographically lies between latitude 06°24'23.36"N and 06°24'30.71"N and between longitude 05°37'52.64"E and 05°38'3.80"E (Figures 1a & b). The study area lies within the sub-humid tropical region. Benin City has a mean monthly temperature of 27°C and a mean annual rainfall of over 2000mm. Benin City occupies a lowland plain in the south and rises slowly to the Esan Plateau towards the north. This region is endowed with fertile soil. The city is underlain by sedimentary formation of the Miocene-pleistocene age often referred to as the Benin Formation. The Benin Formation comprise of mainly consolidated sand and sandy clays covering the whole of the Niger Delta [25]. The topography is predominantly uniform, a gently undulating surface area rising from about 505m in the south-eastern parts to about 215m in the northern parts giving a mean elevation of about 83m above sea level. Temperature values in the area are usually on the high side throughout the year with a minimum annual temperature of 21.9^0C and a mean annual maximum temperature of 25.1^0C.

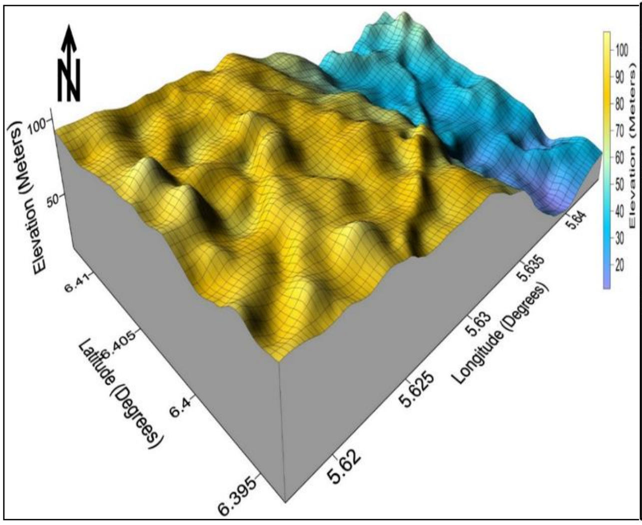

Fig. 1a. 3D Imagery of configuration of the study

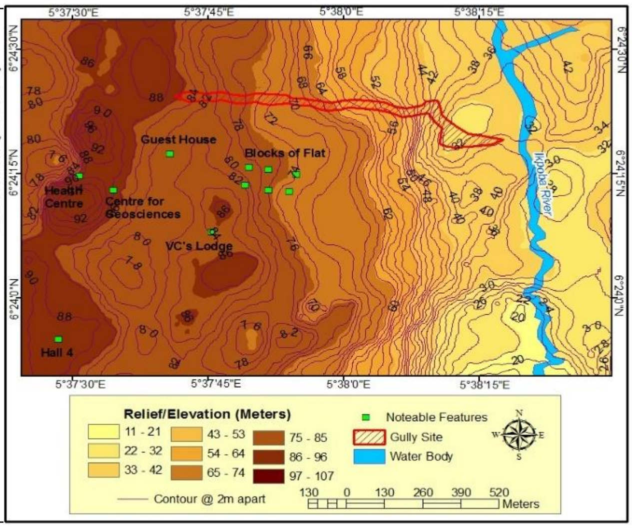

Fig. 1b. Topography of the study area and Gully

2.2 Data collection

To estimate rainfall erosivity values for the study area, monthly rainfall data were collected from the office of Nigeria Meteorological Agency for a period of 19years (2000-2018). To supplement the monthly rainfall, daily rainfall data were collected from the National Centre for Energy and Environment, University of Benin. To collect soil samples, points were established along the gully site. The chainage points were measured at 150-metre (m) intervals to a depth of 30cm. The width of the gully at the chainage point was measured. A control point was established at the centre of each chainage point and at equi-distance from the centre. Then samples were collected at each control using the hand auger at a depth of 0.3metres (m). The hand auger was tampered using the tampering rod in order to loosen the sample from the auger. The samples collected were put into cellophane bags in order to avoid loss of the sample during transportation to the Geotechnical Laboratory of the Civil Engineering Department of the University of Benin for analysis. A total of fifteen (15) samples were collected from the gully sites with point geographical locations, three at each chainage point (Table 1 and Figure 2).

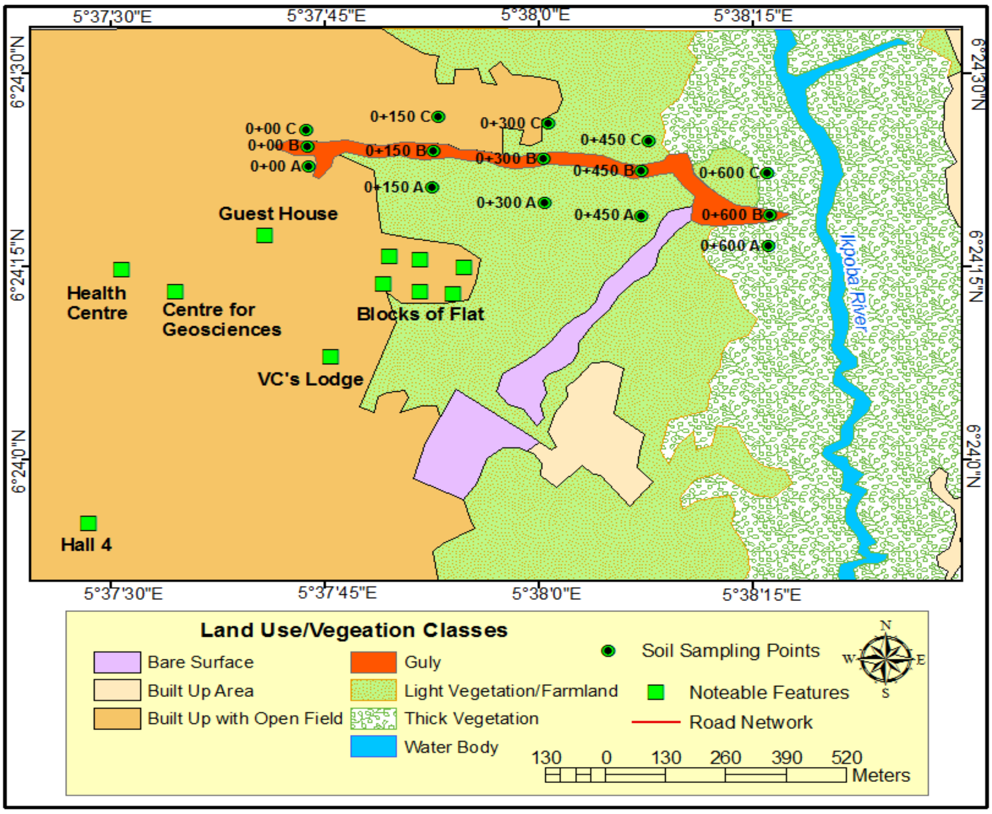

Fig 2: Layout of the study area and soil sampling points

Table 1: Geo-referenced Data of Soil Samples

Chainage	Points	Distance Between Points (m)	Northings	Eastings	Latitude	Longitude
	A	10.00	06°24'23.334"	05°37'52.416"	6.40648	5.63123
0+00	B	10.00	06°24'23.352"	05°37'52.651"	6.40649	5.63129
	C		06°24'23.180"	05°37'52.038"	6.40644	5.63112
	A	8.65	06°24'22.272"	05°37'56.989"	6.40619	5.63250
0+150	B	8.65	06°24'22.950"	05°37'55.077"	6.40638	5.63197
	C		06°24'22.380"	05°37'56.874"	6.40622	5.63246
	A	13.00	06°24'22.746"	05°38'02.004"	6.40632	5.63389
0+300	B	13.00	06°24'22.722"	05°38'01.914"	6.40631	5.63386
	C		06°24'22.296"	05°38'01.830"	6.40619	5.63384
	A	14.50	06°24'22.350"	05°38'06.066"	6.40621	5.63502
0+450	B	14.50	06°24'22.434"	05°38'05.898"	6.40623	5.63497
	C		06°24'21.720"	05°38'05.982"	6.40603	5.63500
	A	16.00	06°24'30.696"	05°38'14.891"	6.40853	5.63747
0+600	B	16.00	06°24'29.752"	05°38'03.802"	6.40827	5.63439
	C		06°24'23.262"	05°38'10.608"	6.40646	5.63628

2.2.1 Vegetation and Land use/Land cover (LU/LC) Maps

January 2017 Landsat TM imagery of Benin City was downloaded from United States Geological Surveys (USGS) website, Google Earth Pro Desktop, exported to Arc Map 10.3 environment and geo-referenced using Latlon Geographic Coordinate System (LGCS). This was followed by on-screen digitization, shape file creation and attribute table for the different vegetation/land use classes. Symbolization was then applied and final vegetation/land use land cover map compiled. The dataset which comes with elevation values expressed in meters was downloaded from USGS website. It has a spatial resolution of 30 by 30 meters and comes with LGCS. Raster clip tool was used to extract the study area for analysis. The DEM was used in preparation of relief, contour, slope and three dimensional model (3D) of the study area.

2.2.2 Normalized Difference Vegetation Index, NDVI

The NDVI tool in Erdas Imagine 9.2 was used to generate NVDI layer from the January 2017 LandSat TM imagery of the study area. Thereafter, the X & Y coordinates of the soil sampling points were used to extract NDVI values with the aid of extract values to point tool in Arc Map 10.3. The extracted NDVI values were then exported to Microsoft excel for use. The calculated soil texture values with (X,Y) coordinates were exported to Arc Map 10.3 environment and interpolated to produce a smooth surface showing the spatial variation in the study area. Specifically, Inverse Distance Weighted (IDW) tool which used minimum of 12 known points was the interpolation method adopted in Arc Map 10.3. The smooth surfaces generated were reclassified into 9 classes using equal interval classification method in symbol tool. The final maps were then exported in *.tif* format for use.

2.3 Data Analysis

The Revised Universal Soil Loss Equation, RUSLE was utilized to determine the annual soil loss across the study area. The equation is given as;

$$A = \boldsymbol{R \cdot K \cdot LS \cdot C \cdot P} \quad (1)$$

where A is the computed Soil Loss, K is the Soil erodibility factor, R is the Rainfall-Runoff Erosivity factor, L is the Slope Length factor, S is the Slope Steepness factor, C is the Cover Management factor, and P is the Support Practice factor.

2.3.1 Laboratory Testing and Analysis of Collected Soil Samples

The soil samples were taken to the Geotechnical Engineering unit of the Civil Engineering Departmental laboratory, University of Benin. All the laboratory tests were conducted in accordance with the general specification given in the British Standard Specifications B.S 1377: 1990; "Method of Test for Soils for Civil Engineering Purposes". Analyses were carried out for Particle Size Analysis, Soil Permeability Test, and Organic Matter (OM) Content Test. The British Standard (BS) sieves were used to separate these grains into their various sizes. This was then weighed and their percentage weights calculated. The materials and apparatus used for the analysis include BS Sieves, Sensitive Weighing Scale, Wire Brush, Pan, Electric Oven, Metal Tray, Sample Containers of Known Weights, Trowel and Distilled Water.

To determine the portion of the soil which passes through a No. 200 (0.075 mm) sieve, the hydrometer method of analysis proposed by John Bouyoucos in 1936 was adopted. The percentage silt and percentage clay is given by the following;

$$\textbf{Percent Silt}, \%\textbf{Silt} = \left(\frac{(H' + \theta')}{Wt.of\ Sample} \times \mathbf{100}\right)\% \quad \textbf{(2)}$$

$$\textbf{Percent Clay}, \%\textbf{Clay} = \left(\frac{(H'' + \theta'')}{Wt.of\ Sample} \times \mathbf{100}\right)\% \qquad \textbf{(3)}$$

Where $(H' + \theta')$ and $(H'' + \theta'')$ are the Corrected Hydrometer Readings at 30 seconds and 8 hours respectively; H' and H'' are the Hydrometer Readings at 30 seconds and 8 hours respectively, and θ' and θ'' are the Temperature Coefficients for H' and H'' respectively. θ' and θ'' are given as:

$$\theta' = (T' - 19.4) \times 0.3 \qquad \textbf{(4)}$$

$$\theta'' = (T'' - 19.4) \times 0.3 \qquad \textbf{(5)}$$

Where T' and T'' are the Temperatures during the Hydrometer Readings, H' and H''.

2.3.1.1 Soil Permeability Test

An indirect method (Allen Hazen formula published in 1893) was used to determine the soil permeability due to the unavailability of the laboratory apparatus.

$$\mathbf{P_o} = \left(d_{10}^{\ 2}\right) \qquad \textbf{(6)}$$

Where P_o is the Co-efficient of Permeability of the soil in metre per second (m/s), C is a constant equals to 0.01 and d_{10} is the particle size for which 10% of the material is finer in millimetres. The materials and equipment used in the determination of the soil permeability include, Soil samples; Weighing Scale; British Standard (BS) Sieves No. 8, No. 10, No. 16, No. 30, No. 40, No. 50, No. 70, No. 100 and No. 200 (of sizes 2.36mm, 2.00mm, 1.18mm, 0.60mm, 0.425mm, 0.30mm, 0.212mm, 0.015mm and 0.075mm respectively); Sample Containers of Known Weights, and Pan. Tables 2 and 3 show the categories of soil structure index and categories of soil permeability class/infiltration index respectively, while Fig. 3 is the Textural Triangle [26].

Table 2: Categories of Soil Structure Index

STRUCTURE CATEGORY	SOIL STRUCTURE	PARTICLE SIZE (mm)
1	Very Fine Particles	<1.0
2	Fine Particles	1.0~2.0
3	Medium or Coarse Particles	2.0~10.0
4	Blocks, Shale or Coarse Particles	>10.0

Source: United States department of Agriculture (USDA) [26]. *National soil Handbook)*

Table 3: Categories of Soil Permeability Class/Infiltration Index

Permeability Class/Infiltration Category, P	Infiltration	Permeability, P_o (Infiltration Rate) mm/hr.
1	Very Fast	>125.00
2	Fast	62.50~125.00
3	Medium	20.00~62.50
4	Medium to Slow	5.00~20.00
5	Slow	1.25~5.00
6	Very Slow	<1.25

Source: adapted from USDA [27]

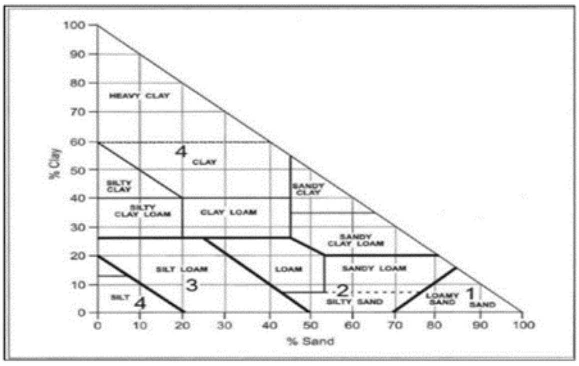

Figure 3 Percentage Clay Vs Percentage Sand Textural Triangle USDA [27]

2.3.2 Organic Mater (OM) Content Test

50grams (g) of the soil sample was collected and entered into the laboratory. The samples were sorted out and rearranged according to laboratory coding. The samples were taken using a spatula and ground to powder using the mortar and pestle. 0.5g of the grinded soil sample was weighed into 250ml conical flask. 5ml of 1 normal Potassium Dichromate, $K_2Cr_2O_7$ (prepared by dissolving

49.03g of the crystal salt in distilled water) was added and the flask swirled. 10ml of Conc. Sulphuric Acid (Tetraoxosulphate VI Acid), H_2SO_4 was added to the sample and the sample further swirled for even reaction and distribution of heat. After swirling the sample was kept on the bench for one hour to allow for a complete reaction. After one hour, 60ml of distilled water was dispensed into the conical flask. Six (6) drops of Diphenylamine Indicator was dropped into the sample and Ammonium Ferrous Sulphate (Ammonium Iron II Sulphate), $(NH_4)_2$, $Fe(SO_4)_2$, $6H_2O$ was titrated into the sample. Colour change to black was observed and as the titration continued, the colour which was black changed to blue and finally to green which was the endpoint. This procedure was repeated for the remaining samples.

2.3.3 Determination of Soil Erodibility Factor, K Values

Soil erodibility K factor was determined using the Wischmeier and Smith [23] equation. The equation was chosen because the K-factor is a composite parameter representing an integrated mean annual value arising from the soil profile reaction to the processes of soil detachment and the transportation by raindrop impact and surface flow [24]. The algebraic approximation of the nomograph for those cases where the silt fraction does not exceed 70% [23] is given as:

$$K = \frac{2.1 \text{ x } 10^{-4}(12-OM)M^{1.14}+3.25(s-2)+2.5(p-3)}{100} \quad \textbf{(7)}$$

Where K is the Soil Erodibility Index in imperial units of ton · acre · hour per hundreds of acre per feet per ton per inches [ton·acre·hr/(100acre·ft.·ton·in)] which can be multiplied by 0.137 when converting into metric system with unit of ton · hectare · hour per hectare per Mega-Joules per millimeter [ton·ha·hr/(ha·MJ·mm)], namely,

$$K \ (in\ metrics) = \frac{K'}{0.1317} \quad \textbf{(8)}$$

M is the portion of silt and very fine sand given as the product of the primary particle size fractions and represented as:

$$M = [\%modified\ silt\ (or\ the\ 0.002\ to\ 0.1\ mm\ size\ fraction)]x\ [\%silt + \%\ sand] \quad \textbf{(9)}$$

OM is the percentage of Organic Matter; S is the Soil Structure Class or Index, and P is Soil Permeability or Soil Infiltration Index [23] (Figure 3). The structure and permeability classes and groups of classes were determined from the Soil Survey Manual [27] shown in Tables 2 and 3.

2.3.4 Estimating value of Kinetic Energy

The "erosiveness of storms in the study area was determined as a function of rainfall kinetic energy using the model developed by Kowal and Kassam [28]. The choice of the model was based on the fact that the method was developed using tropical rainfall samples. Besides, its development was based on direct measurements of rainfall kinetic energy with a piezoelectric sensor that can convert impact strain of a rainfall into an electrical signal within the sensing element" [29]. The equation for computing Kinetic energy of rain is given

$$K.E = (41.4\ Ra - 120)\ x\ 103\ [28] \quad \textbf{(10)}$$

Where K.E is rainfall kinetic energy (ergscm-2)
Ra is rainfall amount per storm (mm).

2.3.5 Determination of Rainfall Intensity and Erosivity Index (EI_{30})

R factor is the coefficient of the average erosion by rain (J/m^2). Rain directly impacts the soil surface because its kinetic energy destroys the structure of the soil and brings the soil components in contact with runoff water. In the absence of rainfall intensity data available for most developing countries of which the study area is a part, equations have been developed to determine the RI factor based on by the average yearly or month rainfall amounts. In this study we used that model developed by Arnoldus [30]. The model has been used in Mauritius to calculate rainfall intensity (RI) as follows

$$RI = \sum_{i=1}^{12} \frac{MR^2}{AR} \qquad \textbf{(11)}$$

Where MR is monthly rainfall and AR is the annual rainfall. Then *RI* (Rainfall Intensity) is substituted in the equation to estimate EI_{30}:

$$\mathbf{E1_{30} = 0.0302 \times RI^{1.9}} \qquad \textbf{(12)}$$

Erosivity Value according to Roose [31] *Method*

Roose (1976) method for estimating rainfall erosivity values from rainfall amounts for West African climates was adopted because the climate of the study area suits the climate in which this model was tested on. The equation is given as:

$$\boldsymbol{R = (0.0158P \times I_{30}) - 1.2} \qquad \textbf{(13)}$$

Where R is the index of erosivity in mmh^{-1},
H is rainfall amount (mm) and
I_{30} is rainfall intensity in 30minutes. (Value of I_{30} has been computed using equation 11).
The computed rainfall erosivity values for this study were compared with Fournier [32]'s Rainfall Aggressivity Index (RAI) modified by Arnoldus [30].

2.3.1.6 Determination of Topographic Factor, LS Values
The LS factor accounts for the effect of topography on erosion in RUSLE and it combines L and S which are the effects of hillslope-length factor and hillslope-gradient factor respectively. The slope length, L factor is computed using the formula below.
Revised Universal Soil Loss Equation, RUSLE [33].

$$\boldsymbol{L = \left(\frac{l}{22.13}\right)^{m}} \qquad \textbf{(14)}$$

Where $\boldsymbol{l}$ is Slope Length, in metres (m) and $\boldsymbol{m}$ is 0.5 if the percent slope is 5 and more; 0.4 if the percent slope is between 3 and 5; 0.3 if percent slope is between 1 and 3, and 0.2 if the percent slope is less than 1. LS is calculated by multiplication of L and S.
Where $\boldsymbol{m}$ is given as

$$\boldsymbol{m = \frac{\beta}{\beta+1}} \qquad \textbf{(15)}$$

and

$$\boldsymbol{\beta = \left[\frac{\left(\frac{\sin\theta}{0.0896}\right)}{3(\sin\theta)^{0.8}+0.56}\right]} \qquad \textbf{(16)}$$

Now,

$$\boldsymbol{Slope\ Steepness, S\ Factor = 10.8\sin\theta + 0.03}, \quad \text{if } \boldsymbol{s < 9\%}$$
$$\boldsymbol{Slope\ Steepness, S\ Factor = 16.8\sin\theta - 0.5}, \quad \text{if } \boldsymbol{s \geq 9\%}$$

To calculate Slope Length, $\boldsymbol{\ell}$, Slope Angle, $\boldsymbol{\theta}$ and Percent Slope, $\boldsymbol{s}$, the highest point and the lowest point of the slope were selected from the Relief Map. Let the elevation of the highest point be $\boldsymbol{A}$

and the elevation of the lowest point be $\boldsymbol{B}$. The difference in the elevation is given as $|\boldsymbol{AB}|$. Let $\boldsymbol{C}$ be at a horizontal distance of the lowest point of the slope from the highest point of the slope. The horizontal distance of the lowest point from the highest point is given as $|\boldsymbol{BC}|$. The Slope Length, $\boldsymbol{\ell}$ is given by $|\boldsymbol{AC}|$ and the Slope Angle, $\boldsymbol{\theta}$ by $\boldsymbol{A\hat{C}B}$. Note that $|\boldsymbol{AB}|$ is also known as the Rise and $|\boldsymbol{BC}|$ is the Run. From the Relief Map, Elevation of Highest Point, $\boldsymbol{A = 88m}$; Elevation of Lowest Point, $\boldsymbol{B = 32m}$, and the Horizontal Distance between the Highest and Lowest Point, $|\boldsymbol{BC}| = \boldsymbol{1240.853m}$. Now, the Difference between Elevation of Highest Point, $\boldsymbol{A}$ and Elevation of Lowest Point, $\boldsymbol{B}$, $|\boldsymbol{AB}| = (\boldsymbol{88 - 32})\boldsymbol{m} = \boldsymbol{56m}$. Figure 4 shows the nature of the slope of the study area.

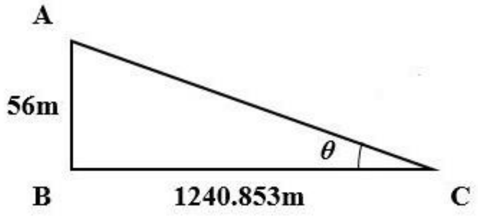

Fig. 4: Nature of Slope in the study area

To determine Slope Length, $\boldsymbol{\ell}$

Note, Slope Length, $\boldsymbol{\ell} = |\boldsymbol{AC}|$

To find $|\boldsymbol{AC}|$

Using Pythagoras' theorem,

$$(|\boldsymbol{AC}|)^2 = (|\boldsymbol{AB}|)^2 + (|\boldsymbol{BC}|)^2 - - - - - - - - - 17$$

Thus, Slope Length, $\boldsymbol{\ell} = |\boldsymbol{AC}| = \sqrt{[(|\boldsymbol{AB}|)^2 + (|\boldsymbol{BC}|)^2]} = \sqrt{(\boldsymbol{56^2 + 1240.853^2})} - -18$

∴ Slope Length, $\boldsymbol{\ell} = |\boldsymbol{AC}| = \boldsymbol{1242.116m}$

To determine Slope Angle, $\boldsymbol{\theta}$

Slope Angle, $\boldsymbol{\theta} = \boldsymbol{A\hat{C}B} = \tan^{-1}\left(\frac{\boldsymbol{RISE}}{\boldsymbol{RUN}}\right) = \boldsymbol{tan}^{-1}\left(\frac{|\boldsymbol{AB}|}{|\boldsymbol{BC}|}\right) = \tan^{-1}\left(\frac{56}{1240.853}\right) = \boldsymbol{2.5840} - - - 19$

∴ Slope Angle, $\boldsymbol{\theta = 2.584^{\circ}}$

To determine Percent Slope, $\boldsymbol{s}$

Percent Slope, $\boldsymbol{s} = \left(\frac{\boldsymbol{RISE}}{\boldsymbol{RUN}} \times \boldsymbol{100}\right)\% = \left(\frac{56}{1240.853} \times \boldsymbol{100}\right)\% = \boldsymbol{4.513\% - - - -20}$

∴ Percent Slope, $\boldsymbol{s = 4.513\%}$

To Compute the Topographic Factor, $\boldsymbol{LS}$.

Recall the Revised Universal Soil Loss Equation, RUSLE (McCool *et al*., 1987)
Slope Length, L Factor = $(L/22.13)^m$ 21

Where $\boldsymbol{m}$ is given as

$$\boldsymbol{m} = \frac{\boldsymbol{\beta}}{\boldsymbol{\beta+1}} - - - - - - - - - - - - - - - - - - \boldsymbol{22}$$

and

$$\boldsymbol{\beta} = \left[\frac{\left(\frac{\sin\boldsymbol{\theta}}{\boldsymbol{0.0896}}\right)}{\boldsymbol{3(\sin\theta)^{0.8} + 0.56}}\right] - - - - - - - - \quad \boldsymbol{23}$$

Now,

$$\boldsymbol{Slope\ Steepness, S\ Factor = 10.8 \sin\theta\ +\ 0.03}, \qquad \text{if } \boldsymbol{s <\ 9\%}$$
$$\boldsymbol{Slope\ Steepness, S\ Factor = 16.8 \sin\theta\ -\ 0.5}, \qquad \text{if } \boldsymbol{s\ \geq\ 9\%}$$

Where,
ℓ is the Slope Length; θ is Slope Angle in degrees and s is the Percent Slope.

From Eq. 18

$$\boldsymbol{\beta = \left[\frac{\left(\frac{\sin\theta}{0.0896}\right)}{3(\sin\theta)^{0.8} + 0.56}\right] = \left[\frac{\left(\frac{sin\,2.584°}{0.0896}\right)}{3(sin\,2.584\,°)^{0.8} + 0.56}\right] = 0.6215}$$

Now,

$$\boldsymbol{m = \frac{\beta}{\beta + 1} = \frac{0.6215}{0.6215 + 1} = 0.3833}$$

Thus,

$$\boldsymbol{lope\ Length, L\ Factor = \left(\frac{\ell}{22.13}\right)^{m} = \left(\frac{1242.116}{22.13}\right)^{0.3833} = 4.6823}$$

$$\therefore\ \boldsymbol{Slope\ Length, L\ Factor = 4.68}$$

Since Percent Slope, $\boldsymbol{s = 4.513\%\ < 9\%}$,

$$\boldsymbol{Slope\ Steepness, S\ Factor = 10.8 \sin\theta\ +\ 0.03}$$
$$\boldsymbol{= 10.8 \sin(2.584°)\ +\ 0.03\ = 0.5169}$$
$$\therefore \boldsymbol{Slope\ Steepness, S\ Factor = 0.5169}$$

Hence, the Topographic Factor, $\boldsymbol{LS = 4.6823\ \times 0.5169 = 2.4202 \cong 2.42}$

$\therefore$ Topographic Factor, $\boldsymbol{LS = 2.42}$

2.3.7 Determination of Cover-Management Factor, C Values

De Jong (1994) derived the following function for estimating the C factor in USLE from Normalized Difference Vegetation Index (NDVI) (revised in De Jong *et al*., 1998):

$$\boldsymbol{C\ =\ 0.431 -\ 0.805(NDVI) - - - - - 24}$$

Where

$$\boldsymbol{NDVI = \left(\frac{RASTERVALUE}{1000}\right) - - - - - - 25}$$

NDVI values range between -1.0 and +1.0. Photosynthetically active vegetation shows a very high reflectance in the near IR portion of the electromagnetic spectrum (Band 4, Landsat 5 TM), in comparison with the visible portion especially red (Band 3, Landsat 5 TM), and hence NDVI values for photosynthetically active vegetation will be very high.

2.3.8 Determination of Support Practice Factor, P Values

The values of the Support Practice factor, $\boldsymbol{P}$ was determined using the relationship between the Land cover and Support Practices factor shown in Table 4.

Table 4: Relationship Between Land Cover and Support Practice Factor, $\boldsymbol{P}$.

Land	P-Factor
Agricultural Land	0.4
Built-up land	1
Tree clad area	0.1
Waste land	1
Water bodies	0.5

(Source: Devatha [35])

3. Results

Results of particle sizes are illustrated in Table 5 and it shows that the soil samples have higher amount of fine particles than coarse particles. Sample UB 0+150 A is observed to have the highest amount of very fine sand particles.

Table 5: Weights of Dry Soil Samples Retained on British Standard (BS) Sieves.

	WEIGHT OF DRY SOIL SAMPLES RETAINED ON SIEVES (g)														
SIEVE SIZE (mm)		SOIL SAMPLES													
	0+00 A	0+00 B	0+00 C	0+150 A	0+150 B	0+150 C	0+300 A	0+300 B	0+300 C	0+450 A	0+450 B	0+450 C	0+600 A	0+600 B	0+600 C
2.360	1.15	6.65	0.68	0.83	1.43	0.42	1.33	3.46	0.73	0.79	2.71	0.33	1.43	0.40	1.21
2.000	0.66	0.94	0.32	0.26	0.72	0.66	0.19	1.06	0.18	0.59	1.14	0.16	0.96	0.51	0.88
1.180	4.82	7.23	5.42	0.87	6.20	3.95	1.33	8.51	1.89	5.45	7.15	1.90	5.44	6.43	5.84
0.600	20.39	26.82	23.46	2.00	25.37	16.09	3.19	26.74	10.00	25.78	24.11	12.78	23.00	32.48	16.02
0.425	10.32	13.94	9.68	1.05	11.51	9.21	1.23	11.09	7.51	12.37	10.71	8.51	10.29	13.65	7.61
0.300	24.51	21.85	27.48	5.71	27.28	27.00	6.30	23.60	27.47	27.96	25.63	24.74	29.74	26.93	15.22
0.212	13.81	9.81	12.66	11.64	12.35	18.83	5.84	10.61	19.85	11.32	12.43	13.68	11.70	9.64	9.62
0.150	5.45	3.05	4.81	8.91	4.72	7.88	3.86	4.22	9.03	3.62	4.17	6.65	3.52	2.78	5.00
0.075	6.45	5.72	4.43	15.73	4.11	7.86	6.25	3.25	11.32	4.61	4.08	9.05	3.29	1.95	10.06

Tables 6-20 show the analysis of the test results obtained from the hydrometer readings of the soil samples. The study considered only the first four hydrometer readings 5secs, 10secs, 15secs, and 30secs, and the last four readings 2hrs, 4hrs, 8hrs and 24hrs in determining the hydrometer analysis. This is because according to John Bouyoucos method, silt is present in the first 40secs while clay is present after 8hrs.

Table. 6: Hydrometer Test Results for UB 0+00 A.

S/N	FIRST FOUR HYDROMETER READING, H' (mm)	TEMPERATURE AT READING, T' (°C)	LAST FOUR HYDROMETER READING, H" (mm)	TEMPERATURE AT READING, T" (°C)	TEMPERATURE COEFFICIENT FOR H', θ' (°C)	TEMPERATURE COEFFICIENT FOR H", θ'' (°C)	(H'+O')	%CLAY (H"+θ'')	%SILT {(H'+θ') − (H"+θ'')}	$100-(\%CL$
1	3.50	26.00	0.80	26.50	1.98	2.13	5.48	2.93	2.55	94.52
2	3.30	26.00	0.60	27.00	1.98	2.28	5.28	2.88	2.40	94.72
3	3.10	26.00	0.40	27.00	1.98	2.28	5.08	2.68	2.40	94.92
4	3.00	26.00	0.20	26.00	1.98	1.98	4.98	2.18	2.80	95.02

Table 7: Hydrometer Test Results for UB 0+00 B.

S/N	FIRST FOUR HYDROMETER READING, H' (mm)	TEMPERATURE AT READING, T' (°C)	LAST FOUR HYDROMETER READING, H" (mm)	TEMPERATURE AT READING, T" (°C)	TEMPERATURE COEFFICIENT FOR H', θ' (°C)	TEMPERATURE COEFFICIENT FOR H", θ'' (°C)	(H'+θ')	%CLAY (H"+θ'')	%SILT {(H'+θ') − (H"+θ'')}	$100-(\%CL$
1	2.00	26.00	0.00	26.00	1.98	1.98	3.98	1.98	2.00	96.02
2	1.50	26.00	0.00	26.00	1.98	1.98	3.48	1.98	1.50	96.52
3	1.00	26.00	0.00	26.00	1.98	1.98	2.98	1.98	1.00	97.02
4	0.05	26.00	0.00	26.00	1.98	1.98	2.03	1.98	0.05	97.97

Table 8: Hydrometer Test Results for UB 0+00 C.

S/N	FIRST FOUR HYDROMETER READING, H' (mm)	TEMPERATURE AT READING, T' (°C)	LAST FOUR HYDROMETER READING, H" (mm)	TEMPERATURE AT READING, T" (°C)	TEMPERATURE COEFFICIENT FOR H', θ' (°C)	TEMPERATURE COEFFICIENT FOR H", θ" (°C)	(H'+θ')	%CLAY (H"+θ")	%SILT {(H'+θ') − (H"+θ")}	100 − (%CL
1	1.80	26.00	0.60	26.00	1.98	1.98	3.78	2.58	1.20	96.22
2	1.60	26.00	0.50	26.50	1.98	2.13	3.58	2.63	0.95	96.42
3	1.50	26.00	0.40	26.50	1.98	2.13	3.48	2.53	0.95	96.52
4	1.30	26.00	0.20	26.00	1.98	1.98	3.28	2.18	1.10	96.72

Table 9: Hydrometer Test Results for UB 0+150 A

S/N	FIRST FOUR HYDROMETER READING, H' (mm)	TEMPERATURE AT READING, T' (°C)	LAST FOUR HYDROMETER READING, H" (mm)	TEMPERATURE AT READING, T" (°C)	TEMPERATURE COEFFICIENT FOR H', θ' (°C)	TEMPERATURE COEFFICIENT FOR H", θ" (°C)	(H'+θ')	%CLAY (H"+θ")	%SILT {(H'+θ') − (H"+θ")}	100 − (%CL
1	14.50	26.00	9.90	26.50	1.98	2.13	16.48	12.03	4.45	83.52
2	14.00	26.00	9.00	26.50	1.98	2.13	15.98	11.13	4.85	84.02
3	13.30	26.00	8.80	26.70	1.98	2.19	15.28	10.99	4.29	84.72
4	13.00	26.00	8.50	26.00	1.98	1.98	14.98	10.48	4.50	85.02

Table 10: Hydrometer Test Results for UB 0+150 B

S/N	FIRST FOUR HYDROMETER READING, H' (mm)	TEMPERATURE AT READING, T' (°C)	LAST FOUR HYDROMETER READING, H" (mm)	TEMPERATURE AT READING, T" (°C)	TEMPERATURE COEFFICIENT FOR H', θ' (°C)	TEMPERATURE COEFFICIENT FOR H", θ" (°C)	(H'+θ')	%CLAY (H"+θ")	%SILT {(H'+θ') − (H"+θ")}	100 − (%CL
1	1.20	26.00	0.00	26.00	1.98	1.98	3.18	1.98	1.20	96.82
2	1.00	26.00	0.00	26.00	1.98	1.98	2.98	1.98	1.00	97.02
3	0.50	26.00	0.00	26.00	1.98	1.98	2.48	1.98	0.50	97.52
4	0.00	26.00	0.00	26.00	1.98	1.98	1.98	1.98	0.00	98.02

Table 11: Hydrometer Test Results for UB 0+150 C

S/N	FIRST FOUR HYDROMETER READING, H' (mm)	TEMPERATURE AT READING, T' (°C)	LAST FOUR HYDROMETER READING, H" (mm)	TEMPERATURE AT READING, T" (°C)	TEMPERATURE COEFFICIENT FOR H', θ' (°C)	TEMPERATURE COEFFICIENT FOR H", θ" (°C)	(H'+θ')	%CLAY (H"+θ")	%SILT {(H'+θ') − (H"+θ")}	100 − (%CL
1	2.50	27.00	0.70	27.50	2.28	2.43	4.78	3.13	1.65	95.22
2	2.30	27.00	0.60	27.50	2.28	2.43	4.58	3.03	1.55	95.42
3	2.00	27.00	0.40	27.50	2.28	2.43	4.28	2.83	1.45	95.72
4	1.90	27.00	0.30	26.00	2.28	1.98	4.18	2.28	1.90	95.82

Table 12: Hydrometer Test Results for UB 0+300 A

S/N	FIRST FOUR HYDROMETER	TEMPERATURE AT	LAST FOUR HYDROMET	TEMPERATURE AT	TEMPERATURE	TEMPERATURE	(H'+θ')	%CLAY (H"+θ")	%SILT	100 − (%CL

	READING, H' (mm)	READING, T' (°C)	ER READING, H" (mm)	READING, T" (°C)	COEFFICIEN T FOR H', θ' (°C)	COEFFICIE NT FOR H", θ" (°C)			{(H'+θ') − (H"+θ")}	
1	27.50	26.00	19.20	27.50	1.98	2.43	29.48	21.63	7.85	70.52
2	27.30	26.00	19.00	27.50	1.98	2.43	29.28	21.43	7.85	70.72
3	27.00	26.00	18.80	27.50	1.98	2.43	28.98	21.23	7.75	71.02
4	26.50	26.00	16.50	26.00	1.98	1.98	28.48	18.48	10.00	71.52

Table 13: Hydrometer Test Results for UB 0+300 B

S/N	FIRST FOUR HYDROMETER READING, H' (mm)	TEMPERATURE AT READING, T' (°C)	LAST FOUR HYDROMETER READING, H" (mm)	TEMPERATURE AT READING, T" (°C)	TEMPERATURE COEFFICIENT FOR H', θ' (°C)	TEMPERATURE COEFFICIENT FOR H", θ" (°C)	(H'+θ')	%CLAY (H"+θ")	%SILT {(H'+θ') − (H"+θ")}	100 − (%CL
1	1.50	27.00	0.00	27.00	2.28	2.28	3.78	2.28	1.50	96.22
2	1.20	27.00	0.00	27.00	2.28	2.28	3.48	2.28	1.20	96.52
3	1.00	27.00	0.00	27.00	2.28	2.28	3.28	2.28	1.00	96.72
4	0.90	27.00	0.00	27.00	2.28	2.28	3.18	2.28	0.90	96.82

Table 14: Hydrometer Test Results for UB 0+300 C

S/N	FIRST FOUR HYDROMETER READING, H' (mam)	TEMPERATURE AT READING, T' (°C)	LAST FOUR HYDROMETER READING, H" (mm)	TEMPERATURE AT READING, T" (°C)	TEMPERATURE COEFFICIENT FOR H', θ' (°C)	TEMPERATURE COEFFICIENT FOR H", θ" (°C)	(H'+θ')	%CLAY (H"+θ")	%SILT {(H'+θ') − (H"+θ")}	00 − (%CLAY
1	2.80	26.00	1.10	26.20	1.98	2.04	4.78	3.14	1.64	95.22
2	2.60	26.00	1.00	26.50	1.98	2.13	4.58	3.13	1.45	95.42
3	2.50	26.00	0.60	27.00	1.98	2.28	4.48	2.88	1.60	95.52
4	2.20	26.00	0.50	26.00	1.98	1.98	4.18	2.48	1.70	95.82

Table 15: Hydrometer Test Results for UB 0+450 A

S/N	FIRST FOUR HYDROMETER READING, H' (mm)	TEMPERATURE AT READING, T' (°C)	LAST FOUR HYDROMETER READING, H" (mm)	TEMPERATURE AT READING, T" (°C)	TEMPERATURE COEFFICIENT FOR H', θ' (°C)	TEMPERATURE COEFFICIENT FOR H", θ" (°C)	(H'+θ')	%CLAY (H"+θ")	%SILT {(H'+θ') − (H"+θ")}	%SAND
1	0.50	26.00	0.00	26.00	1.98	1.98	2.48	1.98	0.50	97.52
2	0.30	26.00	0.00	26.00	1.98	1.98	2.28	1.98	0.30	97.72
3	0.10	26.00	0.00	26.00	1.98	1.98	2.08	1.98	0.10	97.92
4	0.00	26.00	0.00	26.00	1.98	1.98	1.98	1.98	0.00	98.02

Table 16: Hydrometer Test Results for UB 0+450 B

S/N	FIRST FOUR HYDROMETER READING, H' (mm)	TEMPERATURE AT READING, T' (°C)	LAST FOUR HYDROMETER READING, H" (mm)	TEMPERATURE AT READING, T" (°C)	TEMPERATURE COEFFICIENT FOR H', θ' (°C)	TEMPERATURE COEFFICIENT FOR H", θ" (°C)	(H'+θ')	%CLAY (H"+θ")	%SILT {(H'+θ') − (H"+θ")}	100 − (%CL
1	0.00	26.00	0.00	26.00	1.98	1.98	1.98	1.98	0.00	98.02

2	0.00	26.00	0.00	26.00	1.98	1.98	1.98	1.98	0.00	98.02
3	0.00	26.00	0.00	26.00	1.98	1.98	1.98	1.98	0.00	98.02
4	0.00	26.00	0.00	26.00	1.98	1.98	1.98	1.98	0.00	98.02

Table 17: Hydrometer Test Results for UB 0+450 C

S/N	FIRST FOUR HYDROMETER READING, H' (mm)	TEMPERATURE AT READING, T' (℃)	LAST FOUR HYDROMETER READING, H" (mm)	TEMPERATURE AT READING, T" (℃)	TEMPERATURE COEFFICIENT FOR H', θ' (℃)	TEMPERATURE COEFFICIENT FOR H", θ" (℃)	(H'+ θ')	%CLAY (H"+ θ")	%SILT {(H'+ θ') − (H"+ θ")}	100 − (%CL
1	5.00	26.00	2.20	26.50	1.98	2.13	6.98	4.33	2.65	93.02
2	5.30	26.00	2.00	27.00	1.98	2.28	7.28	4.28	3.00	92.72
3	5.10	26.00	1.80	27.00	1.98	2.28	7.08	4.08	3.00	92.92
4	4.00	26.00	1.50	26.00	1.98	1.98	5.98	3.48	2.50	94.02

Table 18: Hydrometer Test Results for UB 0+600 A

S/N	FIRST FOUR HYDROMETER READING, H' (mm)	TEMPERATURE AT READING, T' (℃)	LAST FOUR HYDROMETER READING, H" (mm)	TEMPERATURE AT READING, T" (℃)	TEMPERATURE COEFFICIENT FOR H', θ' (℃)	TEMPERATURE COEFFICIENT FOR H", θ" (℃)	(H'+ θ')	%CLAY (H"+ θ")	%SILT {(H'+ θ') − (H"+ θ")}	100 − (%CL
1	0.80	26.00	0.00	26.50	1.98	2.13	2.78	2.13	0.65	97.22
2	0.50	26.00	0.00	26.50	1.98	2.13	2.48	2.13	0.35	97.52
3	0.00	26.00	0.00	26.00	1.98	1.98	1.98	1.98	0.00	98.02
4	0.00	26.00	0.00	26.00	1.98	1.98	1.98	1.98	0.00	98.02

Table 19: Hydrometer Test Results for UB 0+600 B

S/N	FIRST FOUR HYDROMETER READING, H' (mm)	TEMPERATURE AT READING, T' (℃)	LAST FOUR HYDROMETER READING, H" (mm)	TEMPERATURE AT READING, T" (℃)	TEMPERATURE COEFFICIENT FOR H', θ' (℃)	TEMPERATURE COEFFICIENT FOR H", θ" (℃)	(H'+ θ')	%CLAY (H"+ θ")	%SILT {(H'+ θ') − (H"+ θ")}	100 − (%CL
1	0.05	26.00	0.00	26.00	1.98	1.98	2.03	1.98	0.05	97.97
2	0.00	26.00	0.00	26.00	1.98	1.98	1.98	1.98	0.00	98.02
3	0.00	26.00	0.00	26.00	1.98	1.98	1.98	1.98	0.00	98.02
4	0.00	26.00	0.00	26.00	1.98	1.98	1.98	1.98	0.00	98.02

Table 20: Hydrometer Test Results for UB 0+600 C

S/N	FIRST FOUR HYDROMETER READING, H' (mm)	TEMPERATURE AT READING, T' (℃)	LAST FOUR HYDROMETER READING, H" (mm)	TEMPERATURE AT READING, T" (℃)	TEMPERATURE COEFFICIENT FOR H', θ' (℃)	TEMPERATURE COEFFICIENT FOR H", θ" (℃)	H'+ θ')	%CLAY (H"+ θ")	%SILT {(H'+ θ') − (H"+ θ")}	100 − (%CL
1	10.50	26.00	6.00	26.50	1.98	2.13	12.48	8.13	4.35	87.52
2	10.00	26.00	5.40	26.50	1.98	2.13	11.98	7.53	4.45	88.02
3	9.50	26.00	5.00	26.70	1.98	2.19	11.48	7.19	4.29	88.52

4	9.30	26.00	4.60	26.00	1.98	1.98	11.28	6.58	4.70	88.72

Table 21, shows the d_{10} values, the values of the coefficient of permeability of soil samples in metre per second m/s and millimetre per hour mm/hr., and their permeability class. It was observed that soil samples have very high infiltration rate, ranging from 93.64 - 2509.06 mm/hr; a characteristic of sandy soils.

Table 21: d_{10} Values of Soil Samples

SOIL SAMPLES	d_{10}, mm	$(d_{10})^2$, mm^2	P_o, m/s $[= C(d_{10})^2]$	P_o, mm/hr.	PERMEABILITY CLASS, P
0+00 A	0.189	0.035721	0.00035721	1285.956	1
0+00 B	0.063	0.003969	0.00003969	142.884	1
0+00 C	0.218	0.047524	0.00047524	1710.864	1
0+150 A	0.051	0.002601	0.00002601	93.636	2
0+150 B	0.225	0.050625	0.00050625	1822.5	1
0+150 C	0.172	0.029584	0.00029584	1065.024	1
0+300 A	0.09	0.0081	0.000081	291.6	1
0+300 B	0.075	0.005625	0.00005625	202.5	1
0+300 C	0.142	0.020164	0.00020164	725.904	1
0+450 A	0.259	0.067081	0.00067081	2414.916	1
0+450 B	0.264	0.069696	0.00069696	2509.056	1
0+450 C	0.081	0.006561	0.00006561	236.196	1
0+600 A	0.186	0.034596	0.00034596	1245.456	1
0+600 B	0.236	0.055696	0.00055696	2005.056	1
0+600 C	0.097	0.009409	0.00009409	338.724	1

For which $C = 0.01$.

Table 22 shows the percentage of organic carbon (%OC) and organic matter (%OM) in the soil samples. It revealed that the organic matter content in the soil samples is small. This affects the erodibility of the soils as soils with low erodibility may be characterized with low organic matter content.

Table 23 shows the average percentage silt, clay and percentage sand. The results show that sample UB 0+300 A has the largest quantity of clay and silt succeeded by sample UB 0+150 A. However, sample UB 0+150 A has the highest amount of very fine sand. Furthermore, sample UB 0+600 B has the relatively highest amount of sand.

Table 22: Percentage Organic Carbon and Percentage Organic Matter in Soil Samples

SOIL SAMPLES	DEPTH (m)	$\%OC$	$\%OM$ $(= \%OC \times 1.72)$
0+00 A	0.30	0.58	1.00
0+00 B	0.30	0.26	0.45
0+00 C	0.30	0.32	0.55
0+150 A	0.30	0.90	1.55
0+150 B	0.30	0.61	1.05
0+150 C	0.30	0.96	1.65
0+300 A	0.30	1.34	2.30
0+300 B	0.30	0.10	0.17
0+300 C	0.30	0.48	0.83
0+450 A	0.30	0.48	0.83
0+450 B	0.30	0.32	0.55
0+450 C	0.30	1.38	2.37
0+600 A	0.30	0.58	1.00

0+600 B	0.30	0.48	0.83
0+600 C	0.30	0.26	0.45

Table 23: Soil Structure Class, ***S***

SOIL SAMPLES	AVERAGE %CLAY	AVERAGE %SILT	%VERY FINE SAND,VFS (0.02mm-0.1mm)	%SAND (0.1mm-2.0mm)	SOIL STRUCTURE CLASS, ***S***
0+00 A	2.67	2.54	6.45	79.96	1
0+00 B	1.98	1.14	5.72	83.64	1
0+00 C	2.48	1.05	4.43	83.83	1
0+150 A	11.16	4.52	15.73	30.44	3
0+150 B	1.98	0.68	4.11	88.15	1
0+150 C	2.82	1.64	7.86	83.62	1
0+300 A	20.69	8.36	6.25	21.94	3
0+300 B	2.28	1.15	3.25	85.83	1
0+300 C	2.91	1.60	11.32	75.93	1
0+450 A	1.98	0.23	4.61	87.09	1
0+450 B	1.98	0.00	4.08	85.34	1
0+450 C	4.04	2.79	9.05	68.42	2
0+600 A	2.06	0.25	3.29	84.65	1
0+600 B	1.98	0.01	1.95	92.42	1
0+600 C	7.36	4.45	10.06	60.19	2

Table 24 shows the erodibility factor in metrics, also represented in Figure 5. It was observed that soil erodibility ranges from 0.002 to 0.01ton·ha·hr/(ha·MJ·mm). This result is due to the soil texture being mainly sandy as sand can be easily detached but does not easily runoff. The higher the *K* value of any soil, the greater its susceptibility to rill and sheet erosion, all other factors being equal. The soil structure, texture, organic matter and permeability are the determinants of *K* values. In general, soils with improved soil structure, higher levels of organic matter, greater permeability, have a greater resistance to erosion and, therefore, a lower *K* value. The presence of very fine sand, silt, and clays with high shrink-swell capacity increases the *K* value whereas sand, loam and sandy loam textured soils are less erodible.

Table 24: Erodibility Factor for University of Benin Gully Site

SOIL SAMPLES	%SILT + VFS	%SAND	***%OM***	PERMEABILITY CLASS, ***P***	SOIL STRUCTURE CLASS, ***S***	ERODIBILITY FACTOR IN METRICS, ***K*** [ton·ha·hr/(ha·MJ·mm)]	ERODIBILITY FACTOR, ***K'*** [ton·acre·hr/(100acre·ft.·ton·in)]
UB 0+00 A	8.99	79.96	1.00	1	1	0.004	0.03037
UB 0+00 B	6.86	83.64	0.45	1	1	0.005	0.03797
UB 0+00 C	5.48	83.83	0.55	1	1	0.004	0.03037
UB 0+150 A	20.25	30.44	1.55	2	3	0.010	0.07593
UB 0+150 B	4.79	88.15	1.05	1	1	0.004	0.03037
UB 0+150 C	9.50	83.62	1.65	1	1	0.004	0.03037
UB 0+300 A	14.61	21.94	2.30	1	3	0.007	0.05315
UB 0+300 B	4.40	85.83	0.17	1	1	0.004	0.03037
UB 0+300 C	12.92	75.93	0.83	1	1	0.005	0.03797
UB 0+450 A	4.84	87.09	0.83	1	1	0.005	0.03797
UB 0+450 B	4.08	85.34	0.55	1	1	0.004	0.03037
UB 0+450 C	11.84	68.42	2.37	1	2	0.008	0.06074

UB 0+600 A	3.54	84.65	1.00	1	1	0.004	0.03037
UB 0+600 B	1.96	92.42	0.83	1	1	0.002	0.01519
UB 0+600 C	14.51	60.19	0.45	1	2	0.008	0.06074

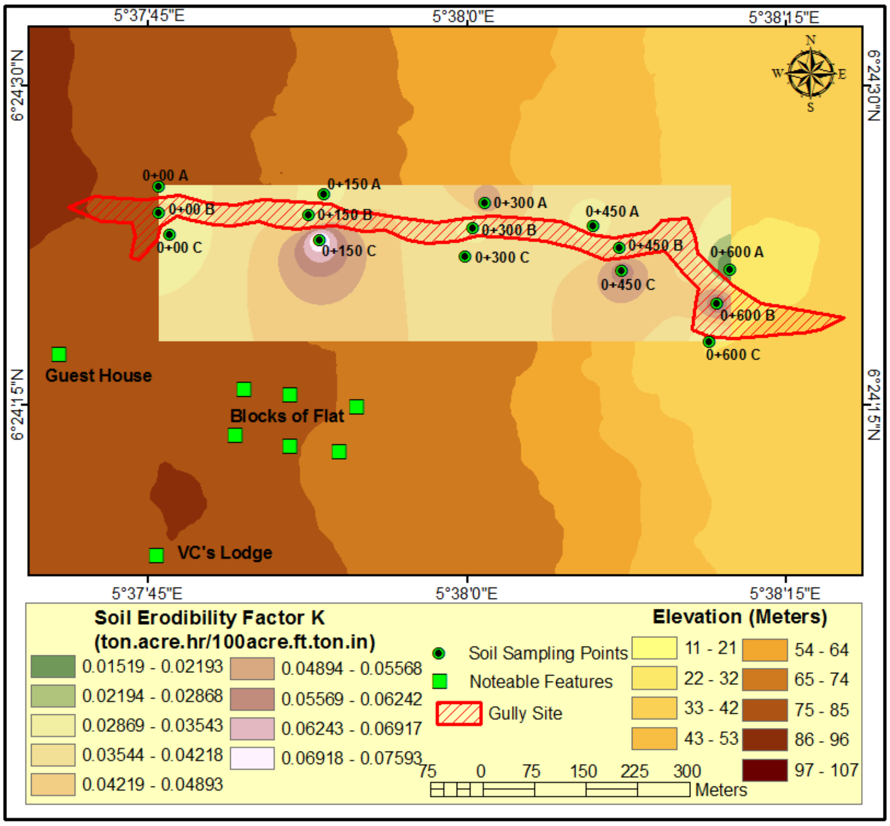

Figure 1: Soil erodibility plot across the study area

Results of rainfall kinetic energy in the study area are presented in Table 25. Rainfall kinetic energy is at peak in July with 124.1MJ/ha and least in January with 4.87MJ/ha. This corresponds with the pattern of rainfall erosivity. The Rainfall-Runoff Erosivity factor, R is estimated using the earlier mentioned formulae. Using Roose Model (MJmm/ha/hr), seasonal Rainfall Erosivity Factor over the study area was also computed and the result is presented in Figure 6. Seasonal erosivity assumes similar pattern with rainfall distribution. The zero value of R in the months of December, January and February is an indication that rainfall during these months are not effective (Figures 7 and 8). On annual basis, the Rainfall-runoff erosivity value for University of Benin is very high when compared to the Rainfall Aggressivity Index proposed by Arnoldus [30] (see Table 26).

Table.25: Kinetic Energy ((MJ/ha)) and Rainfall and Rainfall Erosivity over University of Benin

	Jan	Feb	Mar	Apri	May	June	July	Aug	Sept	Oct	Nov	Dec
KE (MJ/ha)	4.87	18.65	35.63	64.55	81.12	99.47	124.1	120.82	123.75	89.71	24.98	7.6
Rainfall Intensity	0.11	1.18	4.08	13	20.37	30.47	47.2	40.32	46.94	24.85	2.06	0.23
EI_{30} (Jmm $ha^{-1}h^{-1}$)	0	0.04	0.44	0.11	9.27	19.92	45.76	33.92	45.28	13.52	0.12	0

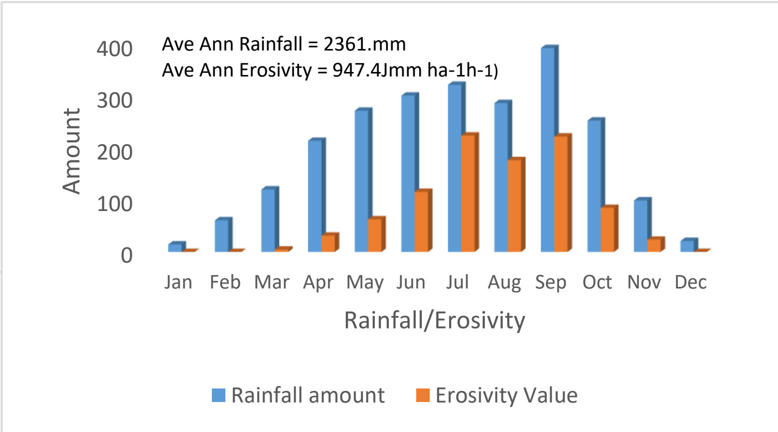

RAINFALL EROSIVITY	Interpretation
0 – 60	Very Low
61 – 90	Low

Tab. 25 Rainfall Aggressivity Index (RAI). (Source: Modified from Arnoldus, [20])

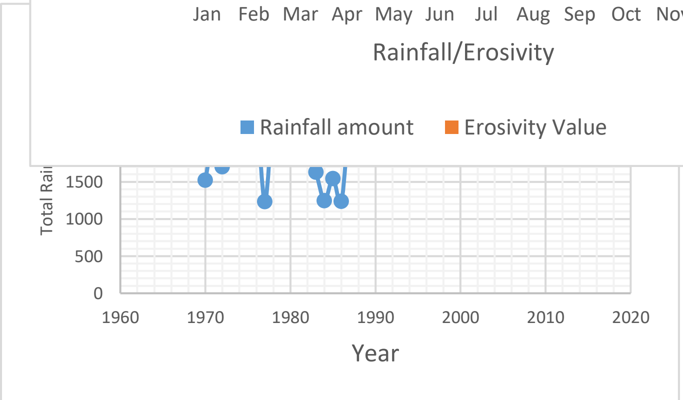

Fig 7: Annual Rainfall Distribution over Benin-City (1970-2012)

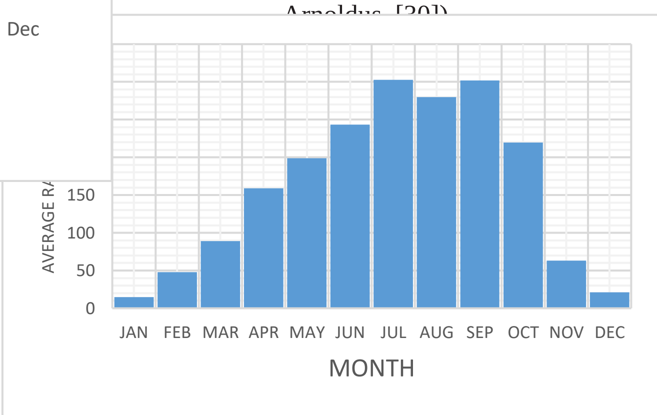

Fig 8: Seasonal Rainfall Distribution over Benin-City (1970-2012)

Our analysis revealed that Benin City experienced the highest rainfall distribution of 3064mm in 2011 and the least of 1234.7mm in 1977. The trend line of the rainfall distribution increased over the years as well as a huge variation in the rainfall distribution. The findings show that Benin City had the least and highest seasonal rainfall distribution in the month of January and July of 14.65mm and 302.65mm respectively.

Using equations 16-23, the computation of LS factor shows that slope length, $\boldsymbol{\ell}$ is 1242.116m; the slope angle, $\boldsymbol{\theta}$ is 2.548° and the percent slope, $\boldsymbol{s}$ is 4.513%. The Slope Length factor, $\boldsymbol{L}$ is 4.6823 and the Slope Steepness factor, $\boldsymbol{S}$ is 0.5169. The combination of the Slope Length factor, $\boldsymbol{L}$ and the Slope Steepness factor, $\boldsymbol{S}$ results in the Topographic factor, $\boldsymbol{LS}$ which has a moderate value of 2.42.

Table 27 shows the Cover Management factor, $\boldsymbol{C}$ and the results revealed that it is uniform throughout the gully site. The Raster value of each sampling point was obtained from the Land Use and Land Cover (NDVI) Map (Figure 9).

Estimated result of soil loss using the RUSLE factors is shown in Table 28 and Figure 10. It revealed that the annual soil loss $\boldsymbol{A}$ over the study area is relatively high with a minimum value of 1.509 ton /ha/yr. and a maximum value of 7.545 ton/ha/yr., and an average value of 4.653 tons/ha/yr. Hence, it can be inferred that soil erosion across the study area ranges from moderate to high around 0+150B where erosion can be said to be young.

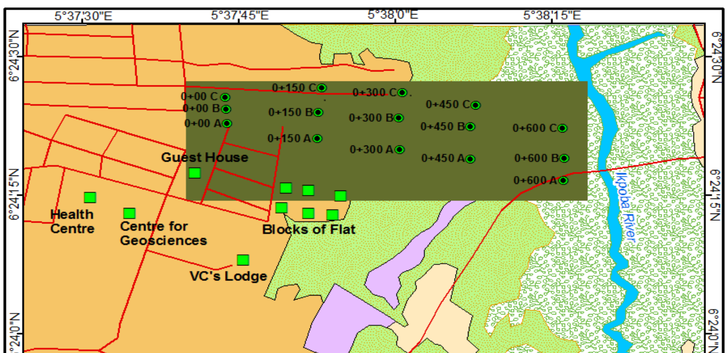

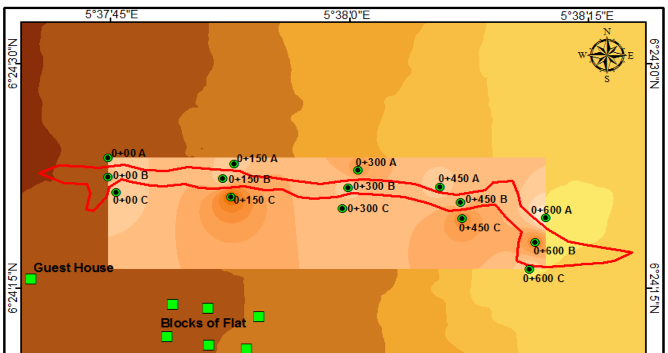

Fig. 9 Normalized Difference Vegetation Index (NDVI). Fig. 10 Soil Loss Map of the University of Benin Gully.

Table 29 shows the width of the gully at the beginning, middle and end of the gully area. The findings show that the gully decreases in width across the chainages as it moves from 0+00 to 0+600. This pattern is expected for a natural erosion cycle with young stage, middle and old stage which are characterized by active erosion, development of well-integrated drainage system and depositional plains respectively as opined by Pimental et al. [36].

Table 27: Table of Cover Management Factor, $\boldsymbol{C}$

SOIL SAMPLES	RASTERVALUE	NDVI $\left(=\frac{RASTERVALUE}{1000}\right)$	COVER MANAGEMENT FACTOR, C
UB 0+00 A	128.00	0.128	0.33
UB 0+00 B	128.00	0.128	0.33
UB 0+00 C	128.00	0.128	0.33
UB 0+150 A	128.00	0.128	0.33
UB 0+150 B	128.00	0.128	0.33
UB 0+150 C	128.00	0.128	0.33
UB 0+300 A	128.00	0.128	0.33
UB 0+300 B	128.00	0.128	0.33
UB 0+300 C	128.00	0.128	0.33
UB 0+450 A	128.00	0.128	0.33
UB 0+450 B	128.00	0.128	0.33
UB 0+450 C	128.00	0.128	0.33
UB 0+600 A	128.00	0.128	0.33
UB 0+600 B	128.00	0.128	0.33
UB 0+600 C	128.00	0.128	0.33

Table 28: Table of Estimated Soil Loss, A

SOIL SAMPLES	ERODIBILITY FACTOR, K [ton·ha·hr/(ha·MJ·mm)]	RAINFALL-RUNOFF EROSIVITY, R [MJ·mm/(ha·hr)]	TOPOGRAPHIC FACTOR, LS	COVER MANAGEMENT FACTOR, C	SUPPORT PRACTICES FACTOR, P	SOIL LOSS, $\boldsymbol{A}$ [ton/ha/yr.]
0+00 A	0.004	944.76	2.42	0.33	1.00	3.018
0+00 B	0.005	944.76	2.42	0.33	1.00	3.772
0+00 C	0.004	944.76	2.42	0.33	1.00	3.018
0+150 A	0.010	944.76	2.42	0.33	1.00	7.545
0+150 B	0.004	944.76	2.42	0.33	1.00	3.018
0+150 C	0.004	944.76	2.42	0.33	1.00	3.018
0+300 A	0.007	944.76	2.42	0.33	1.00	5.281
0+300 B	0.004	944.76	2.42	0.33	1.00	3.018
0+300 C	0.005	944.76	2.42	0.33	1.00	3.772

0+450 A	0.005	944.76	2.42	0.33	1.00	3.772
0+450 B	0.004	944.76	2.42	0.33	1.00	3.018
0+450 C	0.008	944.76	2.42	0.33	1.00	6.036
0+600 A	0.004	944.76	2.42	0.33	1.00	3.018
0+600 B	0.002	944.76	2.42	0.33	1.00	1.509
0+600 C	0.008	944.76	2.42	0.33	1.00	6.036

Table 29: Width of the gully at the beginning, middle and end of the gully area

S/N	LOCATION	CHAINAGE	WIDTH (m)
1	Beginning	0+00	87.361
2	Mid-Section	0+300	28.363
3	End	0+600	84.570

3.2 People's perception of effects of the soil loss and gully erosion over University of Benin

Two hundred respondents who reside within the study area were randomly selected to analyse the effects of the soil loss and erosion over the area, and the respondents identified four (4) effects as shown in Table 30. Among the perceived effects of soil erosion, destruction of infrastructure and abandonment of property such as buildings and roads constitutes the highest (40.5%) with a resultant effect on diminishing aesthetics of the University of Benin. Some buildings around the gully site in the University of Benin are already being threatened as the gully expands (see Plates 1 and 2). Loss of arable land accounted for the second highest (30.5%) effect of soil loss and gully erosion, and 12.5% respondents perceived soil erosion to induce flooding. Flooding is associated with stream pollution and erosion-induced stream pollution is one of the intractable effects of flooding in the study area. Disease outbreak is ranked fifth as an identified effect of soil loss which emanated from washed away sediments from the gully sites. Loss of life was also identified as a potential effect of soil loss and erosion in the University of Benin and this was the least indicated effect with 1% (Table 30).

Table 30: Perceived effects of soil loss and erosion

Effect of soil erosion	Frequency	Percentage	Rank
Destruction of infrastructure and abandonment of property	81	40.5	1st
Loss of arable land	61	30.5	2nd
Flooding	25	12.5	3rd
Stream pollution	18	9	4th
Disease Outbreak	13	6.5	5th
Loss of life	2	1	6th
Total	200	100	

Source: Researcher's computation, 2019

Plate 1: Gully site in University of Benin (see the buildings that are threatened)

Plate 2: Gully site in University of Benin (see the arable land that has been lost)

3.3 Discussion

From the soil analysis, it is observed that the soil of the University of Benin Gully is highly sandy with low clay and silt content with UB 0+300 A having the largest quantity of clay and silt succeeded by sample UB 0+150 A which has a highest amount of very fine sand, and sample UB 0+600 B has the relatively highest amount of sand. The infiltration rate is observed to be very high from the soil permeability test while the organic matter (OM) content of the soil was seen to be very low. The study area was found to be highly erodible, with K value ranging from 0.002 to 0.01 ton·ha·hr/(ha·MJ·mm) due to its soil texture being mainly sandy which makes the soil easily detachable and the high infiltration rate since erodibility is dependent on the texture, organic matter and permeability of the soil. The low organic matter and the fact that the study area has very low clay and silt is attributable to anthropogenic activities such as land use change in the study area. This finding is in agreement with other studies carried out in the humid tropics such as [37-38]. For example study has found that land use change has adverse effects on soil characteristics such as soil texture, permeability and aggregate stability [39]. Changes in the aforementioned soil characteristics are important because change in the rate of soil erodibility emanates from them [40]. Similar studies have also established that land use change from forest to croplands might result in silt and clay increase, and sand decrease [41, 42]. Generally, organic binding agents can significantly enhance the water-stability of aggregates when compared to bare soil or inorganic binding agents [43]. Hence, these organic binding agents play important roles in resistance to soil erosion [44].

Furthermore, it is noticed that rainfall-runoff erosivity value is high for Benin City. Rainfall is the major energy source for detachment and transport of soil particles from the soil profile, thus increasing the erosive power and thereby making small rills converge to form large surface channels; gullies [45-47]. Studies have shown that rainfall is the most important factor that is directly relevant to erosion studies in the tropics [48-52].

Rainfall intensity, duration of fall, drop size, frequency of fall, terminal velocity, annual total amount, kinetic energy among others are the rainfall characteristics that have the ability to loosen up soil structures and consequently detach earth materials from different surfaces [53-55]. Soil erosion is fundamentally initiated by detachment, controlled mostly by shear forces of rainfall drops which is represented by rainfall erosivity factor [56, 57]. The impact energy of raindrop triggers the destruction of aggregates while runoff water transports the detached particles [58]. This has resulted to decreased productivity and sustainability of agriculture [59], degradation of ecosystem function [60, 61], and displacement of human populations [62]. For runoff plots with natural or simulated rainfalls, raindrop energy has been shown to cause a splash crust that modifies the infiltration process and amplifies the runoff importance on the fields; the proportion of rain that cannot infiltrate into the soil is determined by the rainfall intensity in most cases [63, 64]. This runoff starts as a thin trickle of water and picks up energy provided the slope is steep and long enough, and that the notion of a threshold value and duration below which erosion does not occur: a threshold of minimum intensity explained in the erosivity index developed by Hudson [63] and a threshold of duration of high intensity and a duration of the rainfall which causes soil saturation and the disintegration of the soil structure.

In recent years, studies on rainfall extremes analysis and aggressiveness have been carried out across the world [65-69]. “It has been with the advent of mathematical models of soil erosion that rainfall aggressiveness, defined under the name of ‘‘rainfall erosivity R index”, has been systematically analyzed” [29]. The rainfall erosivity factor is one of the six factors in the Universal Soil Loss Equation (USLE) [70] and the Revised Universal Soil Loss Equation (RUSLE) (Renard [24] that is used to compute the ability of rainfall to cause soil loss under different conditions. Thus, it is a method used to predict soil erosion.

The slope angle of the gully is low and the slope length is high, resulting in a relatively moderate topographic factor. The cover management factor of the gully site is relatively low as the gully site is located in an area of little vegetation. From the results, it is discovered that Cover Management factor, C is uniform throughout the gully site. This is expected as the study area has undergone intensive modification in land use arising from expansion in university activities, including residential land use. The soil erosion is strongly related to the land cover and land use [71-74] and land use changes and the percent of vegetation has many effects on soil loss [75-77].

As natural vegetation is modified due to urban expansion, the urban hydrological system has to cope with a highly fluctuating amount of surface runoff water which may become extremely high during periods of rainfall [78]. Hydrological effects of increased impervious surface area typically result in higher flow peaks and larger total streamflow volume, shifts in subsurface flow to surface flow and increases in flood frequency [79-86]. Thus, the higher the flow peaks and larger total streamflow volume as well as increases in flood frequency, the greater the erodibility of soil. Consequently, the annual soil loss was determined to be relatively high having a minimum value of 1.509 ton/ha/yr. and a maximum value of 7.545 ton/ha/yr., with an average value of 4.653 tons/ha/yr. Converting from tons/ha/yr. to kilogram per square kilometre per year (kg/sq. km/yr.), an average of 46.53kg/sq.km of soil is lost in a year from the gully site. This denotes a high amount of soil lost and has resulted in downstream water quality, reduction of landscape productivity and loss of organic matter and nutrients which is in line with findings of Newcombe and Macdonald [87] and Hancock et al. [88]. The Soil loss amount as seen in the study area and its associated impacts will be accelerated by human-induced soil degradation as had been noted by Pimentel et al. [36]; Bai et al. [89]; Ajaero and Mozie [52] and Gelagay and Minale [90]. In addition, respondents' perception of the effects of the soil loss over University of Benin is an indication that the adverse effects of soil loss is already being in the study area.

4. Conclusion and Recommendation

There are variations of soils susceptibility to erosion. The soil erodibility factor K is a measure of erodibility, i.e. the $\boldsymbol{K}$ factor represents both susceptibility of soil to erosion, and the amount and rate of runoff, as measured under the standard unit plot condition. $\boldsymbol{K}$ values of about 0.02 to 0.15 are low and are fine textured soils high in clay and are resistant to detachment. $\boldsymbol{K}$ values of about 0.05 to 0.2 are also low (because of low runoff even though these soils are easily detached) and are coarse texture soils (such as sandy soils). Medium textured soils (such as silt loam soils), have moderate $\boldsymbol{K}$ values of about 0.25 to 0.40, because they are moderately susceptible to detachment and they produce moderate runoff. Soils with high silt content are the most erodible; they tend to crust and produce large amounts and rates of runoff and they are easily detached. From the results it could be established that the soil of the University of Benin Gully is sandy, characterized either as sand or loamy sand. The erodibility of the soil is low ranging from 0.002 to 0.01 ton·ha·hr/(ha·MJ·mm) and the annual soil loss is high ranging from 1.509-7.545 ton/ha/yr. On average, 46.53kg/sq.km of soil is lost in a year from the gully site. This denotes a high amount of soil lost and moderate soil erosion. Destruction of infrastructure and abandonment of property as well as loss of arable land have been identified as the major effects of the gully sites within the University of Benin. Thus, it should be noted that there will be a lot more devastating effects without remediation of the gully site.

The following are the recommendations:

- **i** Conservation planning and land use policies should be developed and implementation of erosion control measures to focus on the more prone slopes that are likely to suffer immensely from the directional influence of rainfall. Various erosion control techniques must be employed concurrently, giving much priority to a more effective and sustainable cover growth on all susceptible slope.
- **ii** Prohibition of refuse dumping along river courses because it impedes the flow of water and causes flooding especially during heavy rainfall.
- **iii** Planting of plantain, banana and grass species such as *Eulaliopsiss binata* (Babiyo), *Neyraudia reynaudiana* (Dhonde), *Cymbopogon microtheca* (Khar) on the floodplains to enhance slope stability and reduce soil erosion.
- **iv** Enlightening the public against location of engineering structures on waterways and enacting a law empowering relevant authorities to prosecute whosoever violates the rule.

References

[1] Butu, A.W., Emeribe, C.N., and Ogbomida E. T (2019): Effects of Seasonal Flooding in Benin City and the need for a Community-Based Adaptation Model in Disaster Management in Nigeria. Nigerian Journal of Environmental Sciences and Technology (NIJEST) 3 (1) , pp 112 – 128

[2] Sigalos, G., Loukaidi, V., Dasaklis, S. and Alexouli-Livaditi, A. (2010). Assessment of the quantity of the Material Transported downstream of Sperchios River, Central Greece. Bulletin of the Geological Society of Greece, 43, 737-745.

[3] Tenaw, M. and Awulachew, S.B. (2009). Soil and Water Assessment Tool (SWAT)-Based Runoff and Sediment Yield Modeling: A Case of the Gumera Watershed in Lake Tana Subbasin Seleshi B. Awulachew, Teklu Er kossa, Vladimir Smakhtin and Ashra Fernando Improved Water and Land Management in the Ethiopian Highlands: Its Impact on Downstream Stakeholders Dependent on the Blue Nile IWMI Subregional Office for East Africa and Nile Basin, Addis Ababa, Ethiopia

[4] Obalum, S.E., Buri, M.M., Nwite, J.C, Watanabe, H.Y., Igwe, C.A and Wakatsuki, T. (2012): Hindawi Publishing Corporation Applied and Environmental Soil Science Volume 2012, Article ID 673926, 10 pages doi:10.1155/2012/673926

[5] Global Soil Partnership (GSP). ISRIC supports the Global Soil PartnershipFood and Agricultural Organization. Regional Office for the Near East and North Africa

[6] Eswarant, H., Lal, R. and Reich, P. F. (2001). Land Degradation. An Overview. United State Department of Agriculture (USDA).

[7] Biggelaar, C.D., Lal, R., Wiebe K., and Breneman, V. (2004). The global impact of soil erosion on productivity. I: absolute and relative erosion-induced yield losses. *Advances in Agronomy, 81*, 1–48

[8] Dregne, H. E. (1990). Erosion and soil productivity in Africa. *Journal of Soil &Water Conservation, 45(4),* 431–436.

[9] FAO (1995). *The conservation and rehabilitation of African lands*. Rome, FAO. 38 pp

[10] Eseigbe, J. O. and Gbakeji, J. O. (2014): Evaluating soil erosion in the Benin metropolis, Edo State, Nigeria. *International Journal of Physical Sciences,* 2(3), 38-45. Available online at http://academeresearchjournals.org/journal/ijps

[11] Mallam, I., Iguisi, E.O. and Tasi'u, Y.R (2016). An Assessment of Gully Erosion in Kano Metropolis, Nigeria. *Global Advanced Research Journal of Agricultural Science,* 5(1), 14-27

[12] Madu, I. and Kundiri, A.M. (2019). Impact of Soil Erosion Predictor Variables on Soil Loss Rates in Biu Area, Borno State, Nigeria. *International Journal of Innovative Research & Development.* 8 (1), 30-36. DOI: 10.24940/ijird/2019/v8/i1/JAN19004

[13] World Bank (1990). *Soil Conservation in Developing Countries: Project and Policy Intervention. Soil Conservation in Developing Countries: Project and Policy Intervention*. Agriculture and Rural Development Department. The World Bank 1818 H Street, NW Washington, DC 20433, USA

[14] Ehiorobo, J.O and Izinyon C.O, (2011). M*easurement and documentation for Flood and Erosion Monitoring and control in the Niger Delta States of Nigeria*, FIG working week 2011

[15] Suraj, S. (1998). Soil Erosion and its economic implication in Kawo, unpublished B.Sc Project Bayero University, Kano.

[16] Shu'aibu, B. (2002). *Effect of gully erosion in Kureke village in Kumbutso Local Government Area Kano State,* unpublished Dissertation Bayero University Kano

[17] Buwa, B. (2003). *Effect of gully erosion in Dukawa Village in Minjibir Local Government Kano State*, unpublished Dissertation Bayero University Kano.

[18] Jeje, L.K. (2005). Urbanization and accelerated erosion: Examples from South Western Nigeria. *Environmental Management Journal*, 2, 1-17.

[19] Warren, A, S.P.J. Batterbury, & H. Osbahr. 2001. Sustainability and Sahelian soils: evidence from Niger. *The Geographical Journal* 167 (4): 324-341

[20] Lal, R. 1995. Erosion-crop productivity relationships for soils of Africa. *Soil Science Society of America Journal*, 59(3), 661-667.

[21] Fistikoglu, O. and Harmancioglu, N.B. (2002). Integration of GIS with USLE in Assessment of Soil Erosion. *Water Resources Management, 16(6),* 447-467.

[22] Bakoariniaina, L.N., Kusky, T., Raharimahefa, T. (2006). Disappearing Lake Alaotra: Monitoring Catastrophic Erosion, Waterway Sitting and Land Degradation Hazards in Madagascar Using Landsat Imagery. *Journal of African Earth Sciences, 44(2),* 241 – 252.

[23] Wischmeier, W. H. and Smith, D.D. (1978). Predicting Rainfall Erosion Losses: A Guide to Conservation Planning. *Agriculture Handbook No. 537. USDA/Science and Education Administration, US. Govt. Printing Office, Washington, District of Columbia, USA.*

[24] Renard, K.G., (1997). Predicting soil erosion by water: a guide to conservation planning with the Revised Universal Soil Loss Equation (RUSLE). United States Government Printing.
[25] Reyment, R.A. (1965). *Aspects of the geology of Nigeria—The Stratigraphy of the Cretaceous and Cenozoic Deposits.* Ibadan University Press, Ibadan.
[26] USDA (1951). *Bureau of Plant Industry, Soils, and Agr. Eng.* Soil Survey Manual.U.S. Gov. Print Office, Washington D.C
[27] U.S. Department of Agriculture (1982) National Resource Inventories Soil Conservation Service, 1984.
[28] Kowal, J. M. and Kassam, A. H. (1976). Energy load and instantaneous intensity of rainstorms at Samaru, northern Nigeria. *Trop. Agric. Met*., 12, 271-280.
[29] Ezemonye, M. N. and Emeribe, C. N. (2012). Rainfall erosivity in Southeastern Nigeria. *Ethiopian Journal of Environmental Studies and Management, 5(2),* 112-122. DOI:http://dx.doi.org/10.4314/ejesm.v5i2.1
[30] Arnoldus, H.M (1980). *An approximation of the rainfall factor in the Universal Soil Loss Equation. In: Assessments of Erosion*, John Wiley and Sons Ltd, 127–132.
[31] Roose, E.J. (1976). *Use of the Universal soil Loss equation to predict erosion in West Africa: Soil Erosion: Prediction and Control*: Soil conservation society of America Ankeny, Lowa
[32] Fournier, F. (1960). *Climat et érosion*. Ed. Presses Universitarires de France. Paris.
[33] McCool, D. K., Brown, L. C., Foster, G. R., Mutchler, C. K., and Meyer, L. D. (1987). Revised Slope Steepness Factor for the Universal Soil Loss Equation. *Transactions of the ASAE, 30(5),* 1387-1396.
[34] De Jong, S.M., Scholte, K., van der Meer, F., Sommer, S. and Lacaze, B. (1998). *The DAIS7915 La Peyne experiment: using airborne imaging spectrometry for land degradation survey and modeling. In: Operational remote sensing for Sustainable Development*. G.J.A. Nieuwenhuis, R.A. Vaughan and M. Molenaar (eds.), A.A. Balkema, Rotterdam: pp. 247-253.
[35] Devatha, C.P., Deshpande, V., Renukaprasad, M.S. (2015). Estimation of Soil loss Using USLE Model for Kulhan Watershed, Chattisgarh- A Case Study. *Aquatic Procedia*, 4, 1429-1436.
[36] Pimentel, D., Harvey, C., Resosudarmo, P., Sinclair, K., Kurz, D., et al. (1995). Environmental and economic costs of soil erosion and conservation benefits. *Science-AAAS-Weekly Paper Edition, 267*, 1117-1122
[37] Szilassi, P., Jordan, G., van Rompaey A., Csillag, G. (2006). Impact of historical land use changes on erosion and agricultural soil properties in Kali Basin at Lake Balaton, Hungary. *Catena,* 68, 96–108.
[38] Emadi, M., Emadi, M., Baghernejad, M., Fathi, H., and Saffari, M. (2008). Effect of land use change on selected soil physical and chemical properties in North Highlands of Iran. J. Applied. Sci., 8(3), 496-502
[39] Emadi, M., Baghernejad, M., Memarian, H.R. (2009). Effect of land-use change on soil fertility characteristics within waterstable aggregates of two cultivated soils in northern Iran. *Land Use Policy*, *26*, 452–457.
[40] Lambin, E.F.; Geist, H.J., (2008). Land-use and land-cover change: local processes and global impacts. *Sci. Business Media*, 1-8.
[41] Bewket, W. and Stroosnijder, L., (2003). Effects of agroecological land use succession on soil properties in Chemoga watershed, Blue Nile basin, Ethiopia. *Geoderma*, 111(1), 85-98
[42] Martinez-Mena, M., Lopez, J., Almagro, M., Boix-Fayos, C. and Albaladejo, J. (2008). Effect of water erosion and cultivation on the soil carbon stock in a semiarid area of South-East Spain. *Soil Tillage Res.*, 99(1), 119-129.
[43] Tisdall, J.M. and J.M. Oades. (1982). Organic matter and water-stable aggregates in soils. *European Journal Soil Science,* 33, 141-163.
[44] Annabi M, Houot S, Francou C, Poitrenaud M, Bissonnais YL. 2007. Soil aggregate stability improvement with urban composts of different maturities. *Soil Science Society of America Journal,* 71, 413–423.
[45] Zachar, D. (1982): *Erosion factors and conditions governing soil erosion and erosion processes*. In: Zachar, D. (Ed.), Soil Erosion. Elsevier Scientific Publishing Company, Amsterdam, The Netherlands, 205–388
[46] Lal, R., (2001). Soil Degradation by Erosion. *Land Degradation and Development* 12(6), 519–539.
[47] Poesen, J., Nachtergaele, J., Verstraeten, G. and Valentin, C. (2003). Gully erosion and environmental change: importance and research needs. *Catena*, 50, 91–133
[48] Young, A. (1972). *Slopes, Geomorphology Text 3*, Edinburgh: Oliver & Boyd, 25-72.
[49] Olson, G.W. (1982). "Opportunities for Improving Land Uses through Soil Survey Interpretations Perspectives", in Prinya, N. (ed.), *First International Symposium on Soils, geology and land Forms/Impact on Land Use Planning in Developing Countries,* Bangkok, Thailand.
[50] FAO (1987). Soil and Water Conservation in Semi-arid Areas. *Soil Bulletin,* 57, 21-98
[51] Jeje, L.K. and Agu, A.N. (1990). Run-off from Bounded Plots in Alakowe in South Western Nigeria, *Applied Geography,* 10, 63-74.
[52] Ajaero, C. K. and Mozie, A.T. (2011). The Agulu-Nanka Gully Erosion Menace in Nigeria: What Does the Future Hold For Population at Risk?" In Leighton, M., Shen, X. and Warner, K. (2011) *Climate Change and Migration: Rethinking Policies for Adaptation and Disaster Risk Reduction*, SOURCE 15/21, UNU-EHS, Bonn, Germany.
[53] Ologe, K.O. (1972). Gullies in the Zaria area: a preliminary study of headscape recession. *Savanna,* 1, 55-66.

[54] Elwell, H.A. and Stocking, M.A (1974). Rainfall parameters and a cover model to predict runoff and Soil loss from grazing land in the arahodesia Sandvels, *Proc. Grassland Soc. Afri*, 9, 157-167.

[55] Oyegun, R.O. (1980). The Effects of Tropical rainfall on Sediment Yield from different land use surfaces in Sub-urban Ibadan. A Ph.D. Thesis submitted to the Department of Geography, University of Ibadan, 21-151

[56] Petkovšek G & Mikoš M (2004) Estimating the R factor from daily rainfall data in the sub-Mediterranean climate of southwest Slovenia / Estimation du facteur R à partir de données journalières de pluie dans le climat sub-méditerranéen du Sud-Ouest de la Slovénie, *Hydrological Sciences Journal*, 49:5, 877, DOI: 10.1623/hysj.49.5.869.55134

[57] Asadi, H., Rouhipour, H., Rafahi, H. Gh. and Ghadiri, H. (2008). Testing a Mechanistic Soil Erosion Model for Three Selected Soil Types from Iran. J. Agr. Sci. Tech., 10(1), 79-91

[58] Roose, E.J. (1975). Application de L' equation de prevision de L' erosion de Wischmeir et smith en Afrique de L' Quest. *Coll. I.I.T.A* Ibadan Nigeria 22pp

[59] Diamond, J. (2005) *Collapse: How Societies Choose to Succeed or Fail*. Viking Press, New York.

[60] Ludwig, J. A. and Tgway, D. J. (2000). Viewing Rangelands as Landscape Systems In: "*Rangeland Desertification*". (Eds.): Arnalds, O. and Archer, S., Kluwer Academic Publishers, Dordrecht, 39–52.

[61] Ludwig, J. A., Eager, R. W., Liedloff, A. C., Bastin, G. N. and Chewings, V. H. (2006). A New Landscape Leakiness Index Based on Remotely Sensed Ground-cover Data. *Ecol. Indicators,* 6, 327–336.

[62] Opie, J. 2000. Ogallala: Water for a dry land. University of Nebraska Press, Lincoln.

[63] Hudson, N.W. (1973). Soil conservation. Ithaca: Cornell University Press.

[64] Angulo-MartínezM, López-VicenteM, Vicente-Serrano SM and Beguería S. 2009. Mapping rainfall erosivity at a regional scale: a comparison of interpolation methods in the Ebro Basin (NE Spain). *Hydrol Earth Syst Sci,* 13, 1907-1920.

[65] Garcia-Oliva, F., Maass, J.M., Galicia, L (1995): Rainstorm analysis and rainfall erosivity of a seasonal tropical region with a strong cyclonic influence on the Pacific Coast of Mexico. *J. Appl. Meteor*. 34, 2491–2498

[66] Sauerborn, P., A. Klein, J. Botschek, and A. Skowronek. 1999. Future rainfall erosivity derived from large-scale climate models: Methods and scenarios for a humid region. Geoderma 93(3-4): 269-276

[67] Easterling, D.R., Evans, J.L., Groisman, Ya, P., Karl, T.R., Kunkel, K.E., Ambenje, P., (2000): Observed variability and trends in extreme climate events: a brief review. Bull. Am. Meteor. Soc. 81, 417–425

[68] Nearing, M.A., Pruski, F.F., O'Neal, M.R., (2004). Expected climate change impacts on soil erosion rates: a review. J. Soil Water Conserv. 59, 43–50

[69] Schutt, B., Schwanghart, W., Ducke, K., Fritzenwenger, G., Husdler, J., Lange, J., Lippitz, A., Lowenhertz, R., Lubnina, T., Marquardt, N., Protze, N., Schimpf, S., Schobrabnski, F., (2007): Field study ''Landscape sensitivity. Landscape sensitivity in the Uguii Nuur catchment, Mongolia, with a special focus on soil erosion. Freie Universitat Berlin, Germany

[70] Wischmeier, W.H., Smith, D.D., Uhland, R.E., 1958. Evaluation of factors in the soil-lossequation. Agric. Eng. 39, 458–462.

[71] Kosmas, C., Danalatos, N.G., Cammeraat, L.H., Chabart, M., Diamantopoulos, J., Farand, R., Gutierrez, L., Jacob, A., Marques, H., Martinez-Fernandez, J., Mizara, A., Moustakas, N., Nicolau, J.M., Oliveros, C., Pinna, G., Puddu, R., Puigdefabregas, J., Roxo, M., Simao, A., Stamou, G., Tomasi, N., Usai, D., Vacca, A., (1997). The effect of land use on runoff and soil erosion rates under Mediterranean conditions. *Catena,* 29, 45–59

[72] García-Ruiz, J.M. (2010). The effects of land uses on soil erosion in Spain: A review. *Catena*, 81, 1-11. doi.org/10.1016/j.catena.2010.01.001

[73] Ranzi, R, Le, T.H. and Rulli, M.C. (2012). A RUSLE approach to model suspended sediment load in the Lo river (Vietnam): effects of reservoirs and land use changes. *J Hydrol*, *422–423*, 17–29

[74] Pacheco, F.A.L., Varandas, S.G.P., Sanches Fernandes, L.F. and Valle Junior, R.F. (2014). Soil losses in rural watersheds with environmental land use conflicts. *Sci Total Environ, 485-486C,*110–120. doi:10.1016/j.scitotenv.2014.03.069

[75] Asselman, N.E.M., Middlekoop, H., and Dijk, P.M., 2003. The impact of changes in climate and land use on soil erosion, transport and deposition of suspended sediment in the River Rhine. *Hydrological Processes*, 17, 3225-3244.

[76] Wijitkosum, S., (2012). Impacts of Land Use Changes on Soil Erosion in Pa Deng Sub-district, Adjacent Area of Kaeng Krachan National Park, Thailand. *Soil and Water Res*.,*7(1),* 10–17.

[77] Zare, M., Panagopoulos, T. and Loures, L. (2017). Simulating the impacts of future land use change on soil erosion in the Kasilian watershed, Iran. *Land Use Policy, 67*, 558-572

[78] Hamdi, R. Termonia, P. and Baguis, P. (2011). Effects of urbanization and climate change on surface runoff of the Brussels Capital Region: a case study using an urban soil-vegetation-atmosphere-transfer model. *Int. J. Climatol.* 31 (13), 1959–1974. DOI: 10.1002/joc.2207

[79] Brun, S. E. and Band, L. E. 2000. Simulating runoff behavior in an urbanizing watershed. Comput. Environ. Urban, 24(1): 5–22. doi:10.1016/S0198-9715(99)00040-X

[80] Hejazi, M.I. and Markus, M. (2009). Impacts of urbanization and climate variability on floods in Northeastern Illinois. *Journal of Hydrological Engineering,* 14, 606–616.

[81] Yang, G., Bowling, L.C., Cherkauer, K.A., Pijanowski, B.C. and Niyogi, D. (2010). Hydroclimatic response of watersheds to urban intensity-An observational and modeling based analysis for the White River basin, Indiana. *Journal of Hydrometeorology,* 11, 122–138.

[82] Hancock, G., Loughran, R., Evans, K. and Balog, R. (2008). Estimation of soil erosion using field and modelling approaches in an undisturbed Arnhem Land catchment, Northern Territory, Australia. *Geographical Research,* 46, 333-349.

[83] Bai, Z.G., Dent, D.L., Olsson, L., Schaepman, M.E. (2008). Proxy global assessment of land degradation. *Soil use and Management,* 24, 223-234.

[84] Gelagay, H.S. and Minale, A.S. (2016): Soil loss estimation using GIS and Remote sensing techniques: A case of Koga watershed, Northwestern Ethiopia. *Int Soil Water Conservation Res.,* 4, 126-136.